

Observations of Electron Diffusion Regions at the Subsolar Magnetopause

F. S. Mozer, S. D. Bale, T. D. Phan, and J. A. Osborne

Space Sciences Laboratory, University of California, Berkeley, California, 94720, USA

(Received 17 June 2003; published 10 December 2003)

Electric and magnetic field observations on the Polar satellite at the subsolar magnetopause show that the magnetopause current is often striated. The largest of the resulting current channels are interpreted as electron diffusion regions because their widths are several electron skin depths and the electron flow U_e within them does not satisfy $\vec{E} + \vec{U}_e \times \vec{B} = 0$. The data suggest that the magnetopause contains many such electron diffusion regions and that they are required because $\vec{E} \times \vec{B}/B^2$ drifting electrons cannot carry the large filamentary currents imposed on the local plasma. The most probable interpretation of $\vec{E} + \vec{U}_e \times \vec{B} \neq 0$ is that the pressure term on the right side of the generalized Ohm's law balances this inequality.

DOI: 10.1103/PhysRevLett.91.245002

PACS numbers: 52.35.Vd, 95.30.Qd, 94.30.Va

Magnetic field reconnection occurs at the interface of two magnetized plasmas that flow towards each other. Reconnection converts the energy stored in the magnetic field into kinetic energy and it modifies magnetic field topologies to allow mass and momentum transfer from one region to the other. Reconnection is known to be the process underlying solar wind-terrestrial magnetosphere interactions and the ensuing internal dynamics of the terrestrial magnetosphere [1] and it is believed to be an agent responsible for particle acceleration on the sun and in the cosmos.

The physics of reconnection occurs on two spatial scales that are associated with the ion and electron dynamics, respectively. On the larger scale of the ion diffusion region, which is c/ω_{pi} (≈ 100 km at the subsolar magnetopause, where c is the speed of light and ω_{pi} is the ion plasma frequency), ions become decoupled from the magnetic field because their fluid velocity \vec{U}_i no longer obeys $\vec{E} + \vec{U}_i \times \vec{B} = 0$, where \vec{E} and \vec{B} are the electric and magnetic fields, respectively. On the smaller scale of the electron diffusion region, which is c/ω_{pe} (≈ 2 km at the subsolar magnetopause, where ω_{pe} is the electron plasma frequency), electrons become decoupled from the magnetic field because $\vec{E} + \vec{U}_e \times \vec{B} \neq 0$.

The efficiency of reconnection is controlled by boundary conditions and by the physics in the electron diffusion region. Historically, the main scientific arguments about reconnection have been less about its existence than about its efficiency [1]. For example, early solar flare theories predicted that reconnection was unimportant because the model of the electron diffusion region assumed in those theories did not allow reconnection at a sufficiently fast rate.

The only prior observation of the electron diffusion region in the magnetosphere is statistical in nature [2]. The purpose of this Letter is to present the first direct observations of electron diffusion regions at the subsolar magnetopause and to shed light on the physical mechanisms associated with their existence

After moving the $(\vec{j} \times \vec{B})$ term from the right to the left side of the generalized Ohm's law [3] and simplifying, it becomes

$$\vec{E} + \vec{U}_e \times \vec{B} \approx -\frac{\vec{\nabla} \cdot \vec{P}_e}{ne} + \frac{m_e}{ne^2} \frac{d\vec{j}}{dt} + \eta \vec{j}, \quad (1)$$

where \vec{U}_e is the velocity of a fluid element of electrons; \vec{j} is the current density; n is the plasma density; \vec{P}_e is the electron pressure tensor, assumed for simplicity to be isotropic; m_e and e are the mass and charge, respectively, of the electron; and η is the resistivity.

This equation describes the fact that the electron diffusion region, which occurs when $\vec{E} + \vec{U}_e \times \vec{B} \neq 0$, is associated with a nonzero divergence of the pressure tensor, inertial effects, and/or resistivity. The nonzero nature of $\vec{E} + \vec{U}_e \times \vec{B}$ and each of the terms on the right-hand side of Eq. (1) will be estimated in the following discussion of three traversals of electron diffusion regions at the subsolar magnetopause by the Polar satellite. Polar is the only satellite that has flown a three-component electric field experiment through the magnetopause to make high time resolution measurements of the electric field (12.5–25 ms) and the plasma density from the spacecraft potential (0.2 s). Such measurements are required to search for electron diffusion regions.

The event of March 31, 2002.—Figure 1 gives 12 s of data during a crossing from the magnetosheath to the magnetosphere, in which the plasma density in panel A decreased from about 10 to 2 cm^{-3} (the dots in each panel represent the actual measurements). The next three panels give the magnetic field in the minimum variance coordinate system in which X is the minimum variance direction and Z is the direction of the reconnecting magnetic field that increased from 0 to about 80 nT, largely in three steps of 10–20 nT each (panel D). These magnetic field steps are rather typical and they signify that the magnetopause current is often striated. Panel F gives the electric field in the Y direction, which was as

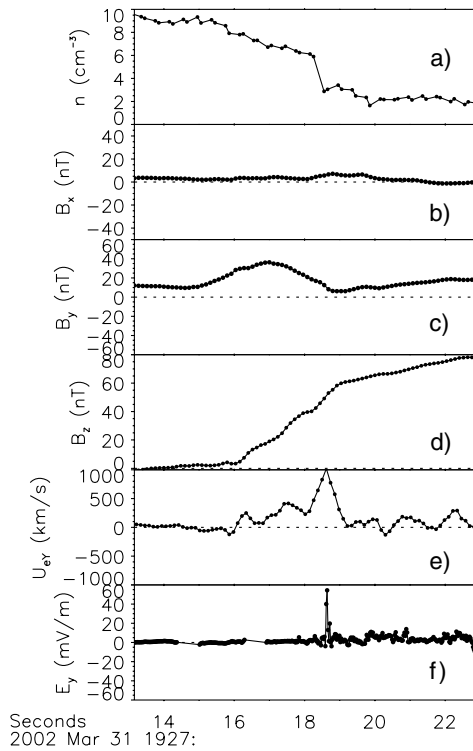


FIG. 1. Plasma density, magnetic, and electric fields measured during a magnetopause crossing from the magnetosheath to the magnetosphere.

large as 60 mV/m in the last current filament. Associated with this current filament, the plasma density decreased by about a factor of 2, as also illustrated in panel A of the 1-s plot in Fig. 2. Such density fluctuations and large electric fields are characteristic features of magnetopause current filaments and they suggest that such large current filaments may be electron diffusion regions. To confirm this association, it is necessary to show both that the size of the current filament is a few times c/ω_{pe} and that $\vec{E} + \vec{U}_e \times \vec{B} \neq 0$.

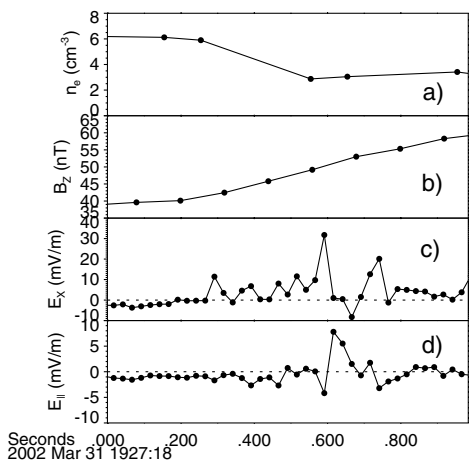


FIG. 2. One second of data during the magnetopause crossing in Fig. 1.

The magnetopause speed, needed to determine the size of this current filament, may be estimated in three ways. The average X component of $\vec{E} \times \vec{B}/B^2$ during this interval was 76 km/s, which suggests a similar magnetopause speed. By noting that E_Y in Fig. 1 was more positive after the magnetopause crossing than before, another estimate of the magnetopause speed may be obtained by transforming to a frame in which the tangential component of the electric field was constant. This gives a magnetopause speed of 46 km/s and a tangential electric field in the magnetopause frame of 0.3 mV/m. Last, the magnetopause speed may be estimated by performing a Faraday residue analysis [4]. For any time interval between 2 and 12 s, this analysis gives a magnetopause speed of 55 km/s within 10 km/s. The speed of 60 ± 15 km/s combines with the 0.2 s duration of the large electric field in panel C in Fig. 2 to yield a thickness of 11 ± 3 km or $(4 \pm 1)c/\omega_{pe}$. (The duration of the electric field signal rather than the duration of the step in the magnetic field is used because the magnetic field data is low-pass filtered, so its rise time is determined by filter characteristics.)

As illustrated in panel D in Fig. 2, there was an apparent parallel electric field as large as 8 mV/m in the current filament. Time resolution issues and measurement errors result in a few mV/m uncertainty in the parallel electric field. Because the measured parallel field is not large compared to this uncertainty, the argument for its existence (and the conclusion that this is an electron diffusion region because $\vec{E} + \vec{U}_e \times \vec{B}$ cannot be zero if there is a parallel electric field) is strengthened by similar parallel field observations in other events.

The flow speed of the current carriers in this filament is estimated by applying Ampere's law to the line integral around a rectangle of width $v_{MP}\Delta t$ in the X direction and height L in the Z direction, where $v_{MP} = 60 \pm 15$ km/s is the magnetopause speed and $\Delta t = 0.2$ s is the time of passage through the large current region. If it is assumed that electrons carry the enhanced current (because the ion gyroradius is much larger than the size of the region), that both the variation of B_X with Z and the displacement current may be neglected, and that the magnetopause crossed the spacecraft at a constant speed in the minimum variance X direction, then Ampere's law yields the estimate of U_{eY} as a function of time that is given in panel E in Fig. 1. It is as large as 1000 km/s because of the large current that the electrons are required to carry in this filament. It may be a factor of 2 greater than this estimate because the low-pass filtering of the magnetic field precludes more rapid changes of B. This large speed also precludes the ions from carrying the current because they would have to be accelerated to ≥ 10 keV, which has not been reported at the magnetopause.

This electron flow speed and the measured fields allow computation of $(\vec{E} + \vec{U}_e \times \vec{B})_X = (E_X + U_{eY}B_Z - U_{eZ}B_Y)$ as a function of time (U_{eZ} has also been computed from Ampere's law by considering a rectangle in the X-Y plane). Figure 3 compares E_X with $U_{eY}B_Z$ and $U_{eZ}B_Y$.

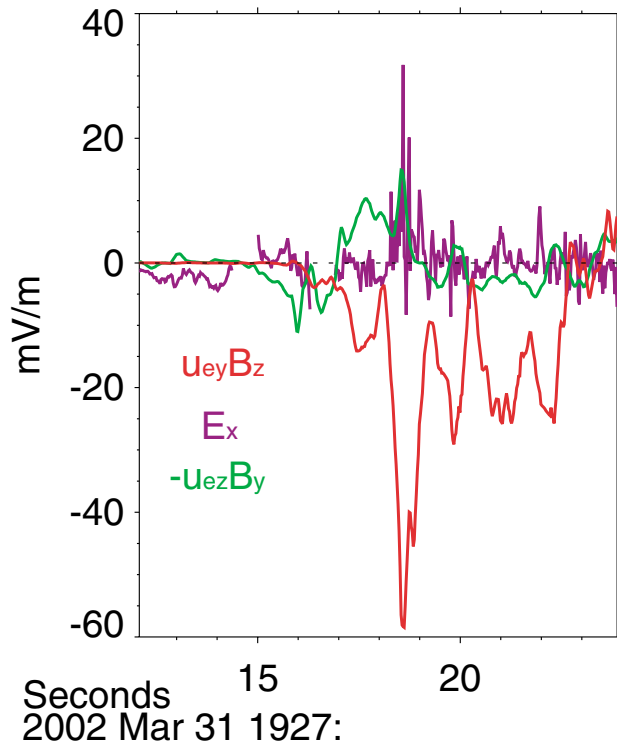


FIG. 3 (color). Components of $(E + U_e \times B)_x$ for the magnetopause crossing in Fig. 1.

The largest value of $|U_{eY}B_Z|$ occurs at the time of the only large E_X . That $|U_{eY}B_Z|$ is significantly larger than $|E_X|$ also shows that this is an electron diffusion region. The deviation of $(\vec{E} + \vec{U}_e \times \vec{B})_X$ from zero is the order of 50 mV/m in the large current region. To examine whether the observed electron density fluctuation can be associated with a pressure gradient of this magnitude, it is assumed that the observed fluctuation is spatial and not temporal. The effective electric field produced by these fluctuations for $(\Delta n/n) \approx -1$ and $kT/e \approx 1000$ V is roughly 50 mV/m. Thus, the pressure gradient term on the right-hand side of Eq. (1) could be large enough to account for the nonzero value of the left-hand side. From the maximum current density of $\approx 10^{-6}$ A/m², which passed over the spacecraft in roughly 200 ms, the convective derivative part of the inertial term on the right-hand side of Eq. (1) is estimated to be more than 2 orders of magnitude too small to contribute to the electron physics.

The event of April 2, 2002.—In Fig. 4, 4 s of data are plotted for a crossing from the magnetosphere, having a plasma density of about 2 cm⁻³ (panel A) and a B_Z of about 60 nT (panel B), to a magnetosheath having a density of about 8 cm⁻³ and $B_Z \approx 0$. B_Z changed in two or three steps with the largest step being about 20 nT in 150 ms (this time comes from the duration of the electric field pulse in panel D). Associated with this current channel there was also a large density fluctuation and a parallel electric field of ≈ 5 mV/m (panel E). The non-zero parallel electric field argues for this being an elec-

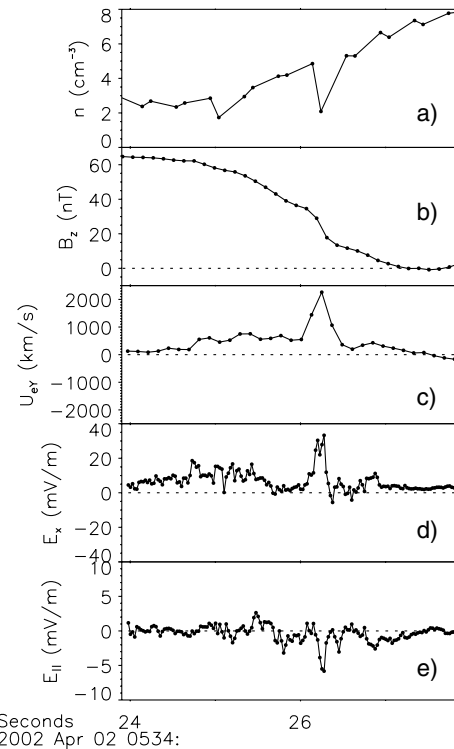


FIG. 4. Plasma density, magnetic, and electric fields measured during a magnetopause crossing from the magnetosphere to the magnetosheath.

tron diffusion region. The electron flow speed required to carry the current associated with the change of B_Z (panel C) was larger than 2500 km/s. During this time interval, the average x component of $\vec{E} \times \vec{B}/B^2$ was -65 km/s. If the magnetopause speed was similar in magnitude, the width of the crossing was about 10 km, or about $4c/\omega_{pe}$. If the density variation was spatial, the effective electric field associated with the pressure gradient may have been as large as 50 mV/m.

The event of March 16, 2003.—Figure 5 presents 5 s of data during an event that occurred when the data transmission rate was at least twice that of the earlier plots. The current channel lasted about 150 ms near 1208:39.6, as measured by the 60 mV/m electric field in panel E. B_Z changed by more than 40 nT during this time (panel C) and there was a major density change (panel A). The electron flow speed required to carry the current in this filament was greater than 1200 km/s (panel D). Because of the higher data rate, the broadband filter channels centered at frequencies of 32, 256, and 2048 Hz (panel F) had sufficient time resolution to measure the wave amplitude within the current channel. The wave power at all frequencies from ≈ 32 to ≈ 2048 Hz was enhanced by more than 20 dB inside the current channel. The 32 Hz channel measures the power at the lower hybrid frequency and that due to a Doppler shifted spatial structure. Near 1208:39, in the high beta region associated with a minimum in the magnetic field intensity (panel B) and as B_Z passed through zero, the wave power

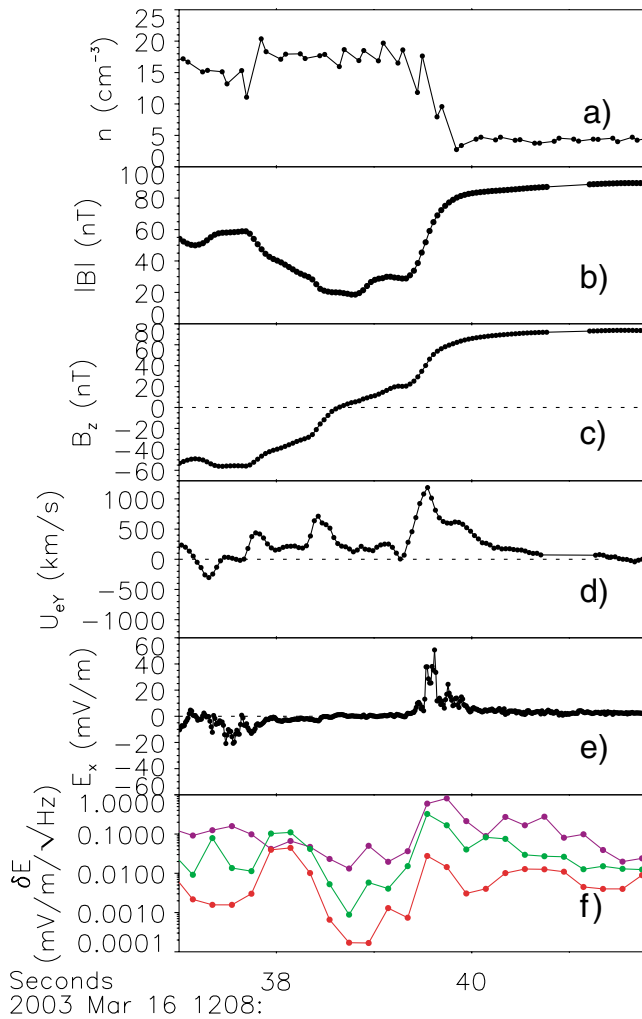


FIG. 5 (color). Plasma density, fields, and wave power measured during a magnetopause crossing from the magnetosheath to the magnetosphere.

was a minimum. This is consistent with results reported by Bale *et al.* [5], which are explained as damping of the wave mode in a high beta plasma.

Discussion.—During a search through approximately 1000 subsolar magnetopause crossings, about 75 examples of apparent electron diffusion regions were found. The presence of parallel electric fields in several cases lends confidence in the measurement and the conclusion that these are electron diffusion regions.

The probability of encountering an electron diffusion region in a single magnetopause crossing is measured to be much greater than that estimated in the popular model of a single electron diffusion region at the X line. This raises the question of the need for or purpose served by such multiple structures. They cannot be required for particle acceleration because $\vec{j} \cdot \vec{E} > 0$ throughout the much larger ion diffusion region. A possible model for understanding why $\vec{E} + \vec{U}_e \times \vec{B} \neq 0$ in several regions

within the magnetopause may be found by considering E_X , $U_{eY}B_Z$, and $U_{eZ}B_Y$, the terms in the X component of this equation. Because the last of these terms is small (as is shown in an earlier example), it is omitted from the following qualitative discussion. If $|E_X| > |U_{eY}B_Z|$, the electron diffusion region may be required because the electric field became too large. This may happen in regions of large and changing currents because the different ion and electron motions that produce the current also produce a local charge separation. A second possibility is that $|U_{eY}B_Z| > |E_X|$, which may happen if the current imposed on the local channel and carried by electrons moving at speed U_{eY} is too large for the electrons to carry while moving with the $\vec{E} \times \vec{B}/B^2$ velocity. This second model better explains the data in Fig. 3.

In summary, the magnetopause may contain many electron diffusion regions at any time. They are associated with filamentary magnetopause currents having widths of several electron skin depths. Within these striated current regions, there are large electric fields both perpendicular and parallel to the magnetic field and large density fluctuations that may be signatures of important pressure gradient terms in the generalized Ohm's law. In the largest current regions, the convective derivative portion of the inertia term in the generalized Ohm's law is too small by more than 2 orders of magnitude to be significant for the electron dynamics. Similarly, although the measured wave power is enhanced inside the electron diffusion region, it is too small by 3 orders of magnitude to influence the electron dynamics, based on a linear theory of anomalous resistivity. However, Vlasov simulations suggest that such an estimate may be low [6]. The observation of small current filaments is consistent with the nonlinear stages of an electromagnetic streaming instability such as the Weibel instability [7,8]. The Weibel instability saturates on spatial scales of c/ω_{pe} , resulting in current filaments that may attract one another and coalesce.

This work was performed under NASA Grant No. NAG5-11733. The authors thank C.T. Russell for the unselfish sharing of his Polar magnetic field data.

-
- [1] G. Haerendel, *The Century of Space Science* (Kluwer Academic, Dordrecht, 2001), p. 1007.
 - [2] J. D. Scudder *et al.*, *J. Geophys. Res.* **107**, 1294 (2002).
 - [3] L. Spitzer, *Physics of Fully Ionized Gases* (Interscience, New York, 1956).
 - [4] A. V. Khrabrov and B. U. Ö. Sonnerup, *Geophys. Res. Lett.* **25**, 2373 (1998).
 - [5] S. D. Bale *et al.*, *Geophys. Res. Lett.* **29**, 2180 (2002).
 - [6] C. E. Watt *et al.*, *Geophys. Res. Lett.* **29**, 1004 (2002).
 - [7] E. W. Weibel, *Phys. Rev. Lett.* **2**, 83 (1959).
 - [8] J.-I. Sakai *et al.*, *Phys. Plasmas* **9**, 2959 (2002).